IEEE Access
Multidisciplinary | Rapid Review | Open Access Journal

Received September 21, 2021, accepted October 21, 2021, date of publication October 26, 2021, date of current version November 9, 2021.

Digital Object Identifier 10.1109/ACCESS.2021.3122883

Investigation of Inner/Outer Rotor Permanent Magnet Flux Switching Generator for Wind Turbine Applications

WASIQ ULLAH, (Graduate Student Member, IEEE), FAISAL KHAN, (Member, IEEE), AND SHAHID HUSSAIN, (Graduate Student Member, IEEE)

Department of Electrical and Computer Engineering, COMSATS University Islamabad, Abbottabad Campus, Abbottabad 22060, Pakistan

Corresponding author: Wasiq Ullah (wasiqullah014@gmail.com)

ABSTRACT In this paper two permanent magnet flux switching generator (PMFSG) is designed for 2 kW output power and 220 V phase voltage at 1500 rpm and comparatively analyzed for wind turbine applications. Both PMFSG share same C-core stator connected back-to-back through flux bridge (β) with different rotor position i.e., inner rotor PMFSG (IR-PMFSG) and outer rotor PMFSG (OR-PMFSG). A detailed comparative analysis with various β for both IR-PMFSG and OR-PMFSG are performed under static characteristics, rated condition, overload capability and over-speed capability for generating output voltage, current, power and efficiency. Comparison of the static characteristics reveal that IR-PMFSG offers 47.93% higher rated power, 2.83% higher efficiency, 22.78% more magnetic flux, 56.91% reduced cogging torque and 83.18% lower torque ripples at the cost of 62.69% higher voltage regulation factor. Furthermore, under rated operating condition and overload capability with same specifications it is found that IR-PMFSG exhibits 1.47 times power than that of OR-PMFSG counterpart. Finally, over-speed capability is investigated in term of the output power which shows that IR-PMFSG significantly generate almost 2.25 time of the specification power whereas OR-PMFSG exhibits nearly 1.25 times power. This analysis shows that IR-PMFSG can be operated at wide-speed rage for higher power specification requirements maintaining efficiency greater than 90%.

INDEX TERMS Flux switching machines, ferrite permanent magnet, inner rotor, outer rotor, wind power generator, wind power application.

I. INTRODUCTION

The potential increase in demand and protection of the environment dominating the net global warming led to increase in development of renewable energy i.e., solar energy, fuel cell, tidal energy, and wind energy. Among the aforesaid renewable energies, wind energy is abundant in nature therefore, in the last few decades the growth and development of wind power generation dominated the net renewable power generating capacity and considered as one of the fastest growing renewable energy sources. In comparison with non-renewable energy, wind energy emerged as most economical and feasible fast-growing renewable energy source for wind power generation with installed capacity of 435 GW by the end of 2015 [1]. This encourages researcher interest in design of wind power generator at various power levels.

Wind power generators adopted numerous types of AC generators such as induction generator, asynchronous generator, permanent magnet (PM) synchronous generator, electrically excited synchronous generator, and PM flux switching generator (PMFSG). Compared with induction generator and electrically excited synchronous generator, PM synchronous generator yield higher energy due to which preferred for wind power applications. Based on PM placement, wind generators are classified as rotor PM generator i.e., surface-mounted PM (SPM) generator and stator PM generator i.e., PMFSG.

Typically, stator PM generator such as PMFSG housed both PM and armature winding on stator leaving a robust simple rotor made of iron [2]–[6]. PMFSG offers high torque density, brushless operation, better voltage regulation, cooling properties, high efficiency, compact stator with passive

The associate editor coordinating the review of this manuscript and approving it for publication was R. K. Saket.

rotor, and sinusoidal back-EMF. In comparison with rotor PM generator i.e., SPM generator with stator PM generator i.e., PMFSG, better temperature dissipation capability is offered in PMFSG due to existence of the thermal sources on stator which ease in cooling hence, risk of irreversible demagnetization is reduced which improve reliability [7]. Furthermore, single tooth non-overlapping concentrated winding owing to smaller mutual flux coupling between adjacent phase winding than distributed winding, therefore, offer good fault tolerant capability [8].

PMFSG exhibits not only high torque density characteristics of PM machines but also offers robust structure like switched reluctance machine to offer elevated torque, reliability, and better speed performance. Therefore, numerous structures have been proposed in the past few decades. A wide range of PM flux switching machines (PMFSMs) are investigated with unique flux nature i.e., axial flux [9] and traverse flux [10] whereas PMFSM with segmented PM consequent pole configuration are thoroughly investigated in [11]–[14]. Besides, flux nature and stator PM magnetization, numerous PMFSM are investigated with different rotor position i.e., inner rotor [15], [16], outer rotor [17], [18], and dual rotor configuration [19], [20] with various stator configuration to achieve maximum power density.

The aforesaid literature investigates different aspects of PMFSG based on the flux nature, PM magnetization and rotor position, however, a detailed comparative study between inner rotor and outer rotor PMFSG in regard of electromagnetic performance for wind power generation is still not reported. Therefore, this paper aims to fulfil this gap through a comparative analysis of inner and outer rotor PMFSG as shown in Figure. 1. The proposed PMFSG is developed by connecting back-to-back C-core stator core with flux bridge so that same stator configuration is utilized for fair comparison. The main purpose of the flux bridge is to provide additional alternate path to magnetic flux. It is worth mentioning that the proposed inner rotor (IR) PMFSG (IR-PMFSG) and outer rotor (OR) PMFSG (OR-PMFSG) share the same stator configuration. Furthermore, the upper slot and lower slot of the stator core are joined with flux bridge which evacuate a portion of the stator core that can be used for cooling purpose. To achieve an optimum flux bridge to join upper and lower slot portion and provide path to the working harmonics content, a detailed investigation is performed on its dimension for better performance.

The rest of article is organized as, section II discusses generator design, section III analyzed static characteristics, Investigation of generator perform is analyzed in section IV and finally some conclusions are drawn in section V.

II. GENERATOR DESIGN

Generator design procedure is different than designing of a motor. In motor design, a predefined maximum torque point under $i_d = 0$ brushless AC operation in considered whereas operating condition of the generator is characterized by external connected load. Furthermore, like motor action

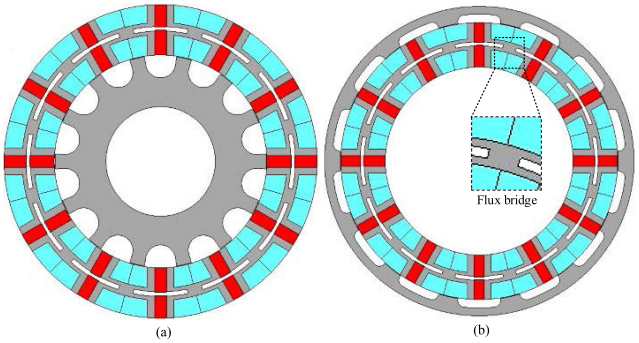

FIGURE 1. Cross sectional view of (a) IR-PMFSG and (b) OR-PMFSG.

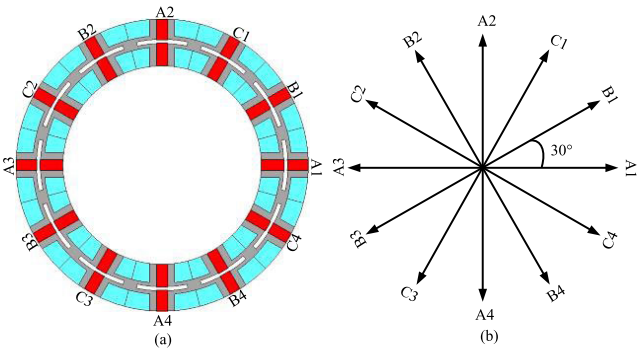

FIGURE 2. Cross sectional view and winding layout (a) stator and (b) Coil and phase EMF phasor.

the applied armature current phase angle is not controllable in case of generator this make generator not feasible for optimization under brushless AC operating mode. Therefore, the power generating performance of generator is determined utilizing a co-simulation method connecting the generator with external circuit. In this regard, power generating performance is thoroughly investigated in the proceeding sections.

Furthermore, to achieve symmetrical phase back electromotive force (EMF) with higher torque density, stator slots and rotor-pole combination are determined. Since both IR-PMFSG and OR-PMFSG share common stator, coils and phase EMF phasor diagram illustrates the phase relation as shown in Figure. 2. The phase shift between two adjacent vector is 30° and distribution factor of 0.966.

Both IR-PMFSG and OR-PMFSG are designed for rated specification power of 2 kW and rated 220 phase voltages at rotor speed of 1500 rpm with the influencing dimensional parameters as illustrated in Figure. 3 and listed in Table 1. Note that both designs are with the same stack length (140 mm), PM volume, and stator outer diameter (210 mm) for fair comparison.

III. STATIC CHARACTERISTICS

Finite element analysis (FEA) based static characteristics of both IR-PMFSG and OR-PMFSG obtained JMAG designer v.20.1 are listed in Table 2 and illustrated in Figure. 4-6 with various flux bridge (β). Variation of the β

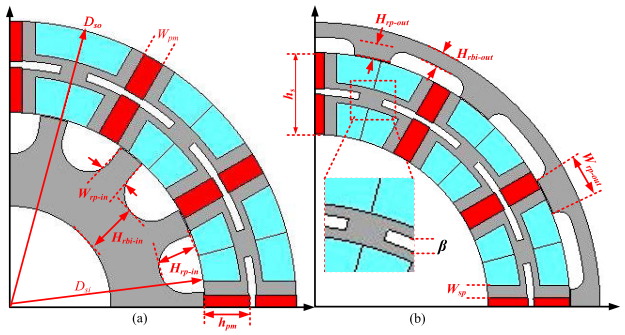

FIGURE 3. Design parameter of (a) IR-PMFSG and (b) OR-PMFSG.

TABLE 1. Leading design parameters of IR-PMFSG and OR-PMFSG.

Symbol	Parameter	Value	Unit
D_{so}	Outer diameter of stator	210	mm
D_{si}	Inner diameter of stator	142.6	mm
h_s	Stator height	33.7	mm
W_{pm}	PM width	8.1	mm
h_{pm}	PM height	15.35	mm
W_{rp-in}	Inner rotor pole width	8.2	mm
W_{rp-out}	Outer rotor pole width	8.2	mm
H_{rp-in}	Inner rotor pole height	14.9	mm
H_{rp-out}	Outer rotor pole height	6	mm
H_{rbi-in}	Inner rotor back iron	34.2	mm
$H_{rbi-out}$	Outer rotor back iron	6	mm
β	Flux bridge	0-3	mm
N_c	Number of turns per phase	50	-
-	PM remanence (Ferrite)	0.4	T
-	Silicon lamination sheets	35H210	-
-	Slot filling factor	0.5	-
L_s	Stack length	25	mm

TABLE 2. Characteristics of IR-PMFSG and OR-PMFSG @ R_{rated}, 1500 RPM and $\beta_{in} = \beta_{out} = 0$.

Characteristics	IR-PMFSG	OR-PMFSG	Unit
Phase back-EMF (rms)	339.9963	266.23	V
Back-EMF THD	8.45	47.57	%
Rated output phase voltage (rms)	234.17	227.82	V
Output phase voltage THD	7.026	15.36	%
Rated output phase current (rms)	4.84	3.36	A
Rated output power	3399	2297.82	W
Voltage regulation factor	45.19	16.86	%
d-axis inductance	0.51	0.69	mH
q-axis inductance	1.19	1.16	mH
d-axis reactance	1.12	1.52	Ω
q-axis reactance	2.62	2.55	Ω
Losses	255.17	242.22	W
Efficiency, η	93.02	90.46	%

for IR-PMFSG is noted with β_{in} whereas for OR-PMFS it is noted with β_{out}. Note that inductance is calculated as per [21], open circuit analysis is performed for phase flux linkage, phase back-EMF and cogging torque whereas brushless AC operation is performed for torque. FEA based analysis as shown in Figure. 4 and Figure. 5 reveals that in comparison with OR-PMFSG, the IR-PMFSG offer more symmetrical and sinusoidal phase flux linkage and phase back-EMF.

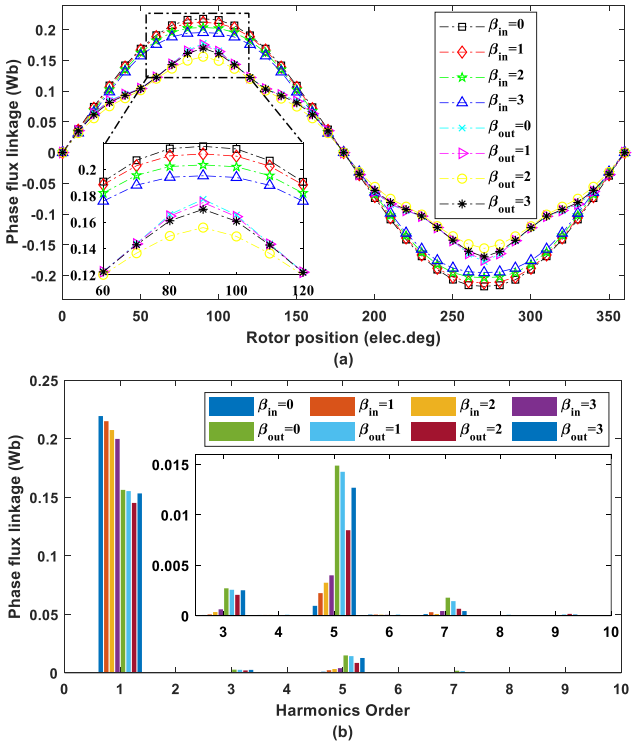

FIGURE 4. Influence of β_{in} and β_{out} on open-circuit performance of IR-PMFSG and OR-PMFSG @ 1500 rpm (a) Phase flux linkage and (b) harmonic spectra.

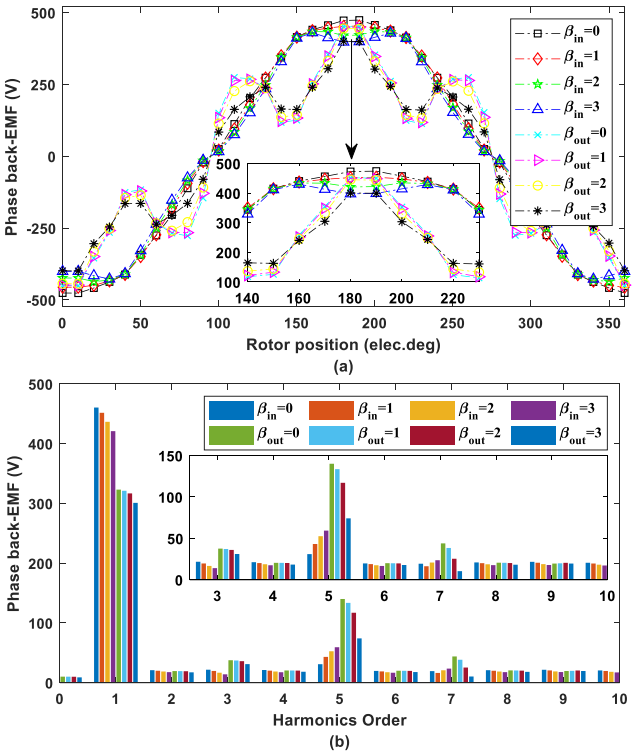

FIGURE 5. Influence of β_{in} and β_{out} on phase back-EMF of IR-PMFSG and OR-PMFSG @ 1500 rpm (a) Phase back-EMF and (b) harmonic spectra.

This is because air-gap magnetic flux density shows major role in modulation effects by salient rotors. The modulation

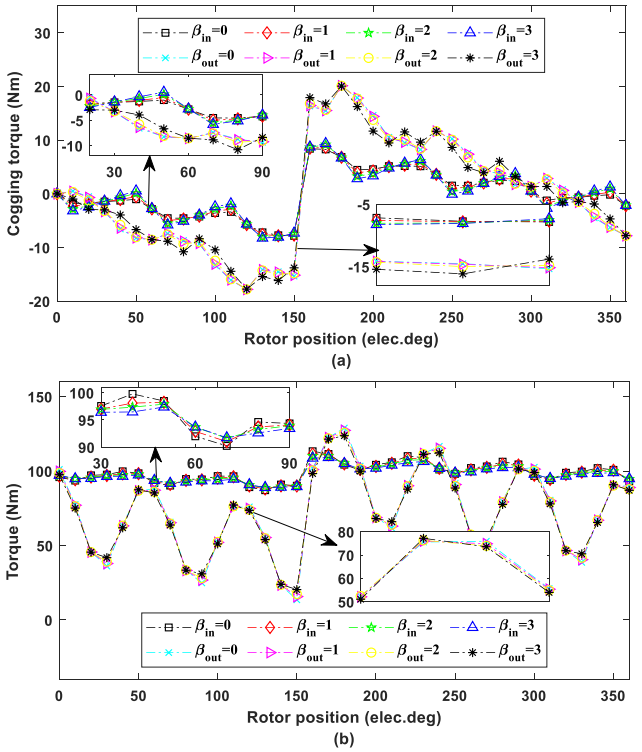

FIGURE 6. Variation of torque performance with β_{in} and β_{out} @ 1500 rpm (a) Cogging torque and (b) Torque (brushless AC operating mode).

phenomena of the salient rotor make field harmonics of the air-gap generated by PM and armature reaction to rotate synchronously to produce torque as shown in Figure. 6. In addition, due to flux focusing effects on IR-PMFSG the magnetic flux density is higher resulting higher torque, power, and efficiency. Comparison of the static characteristics reveals that IR-PMFSG offers 47.93% higher rated power, 2.83% higher efficiency at the cost of 62.69% higher voltage regulation factor.

Comparison of the IR-PMFSG and OR-PMFSG reveals that IR-PMFSG offers 22.78% higher magnetic flux than counterpart. It is noteworthy that when the rotor position from inner is shifted to the outer the influence of dominant harmonics i.e., 3^{th}, 5^{th} and 7^{th} drastically increases. From the quantitative performance as listed in Table 2, it can be clearly seen that back-EMF total harmonic distortion (THD) is increased up to 5.6 times in OR-PMFSG which is mainly due to contribution of higher order harmonics content. Note that with the introduction of β_{in} and β_{out} in stator, the influence of the harmonics content is slightly curtailed. Harmonic spectra as shown in Figure. 4(b) and Figure. 5(b) shows that with the increase in β_{in}, both fundamental and higher order harmonics content tent to decreases whereas with β_{out} the higher order harmonics initially decreases and then increases in phase flux linkage whereas in back-EMF all the higher order harmonics content continue to decrease. This analysis reveals that introduction of the β_{in} and β_{out} greatly helps in THD reduction in phase back-EMF.

Figure. 6 shows cogging torque and electromagnetic torque for both IR-PMFSG and OR-PMFSG with various β_{in} and β_{out}. Quantitative performance analysis reveals that peak to peak cogging torque offered by IR-PMFSG is 16.23 Nm whereas for OR-PMFSG is 37.96 Nm which is 2.34 times of IR-PMFSG that results dominant torque ripples content in electromagnetic torque as shown in Figure. 6(b). Analysis reveals that the torque ripple ratio by OR-PMFSG is 0.264% whereas for OR-PMFSG it is 1.57%. Furthermore, with the introduction of β_{in} and β_{out} torque ripples are slightly curtailed to 1.43% in OR-PMFSG whereas for IR-PMFSG it is reduced to 0.25%. Due to lower cogging torque and torque ripples, IR-PMFSG exhibits lower acoustic noise and vibration in comparison with OR-PMFSG [22].

IV. INVESTIGATION OF GENERATOR PERFORMANCE

On-load generator performance includes output voltage, output current, power, losses, efficiency, and voltage regulation capability when generator is operated with external symmetrical resistive loads. Finite element (FE) based co-simulation is performed to predict generator output phase voltage, output current and losses and based on FE predicted data output power, efficiency and voltage regulation are computed. This analysis is performed on IR-PMFSG and OR-PMFSG under rated performance, overload capability, and over-speed capability.

A. RATED PERFORMANCE

Output phase voltage and phase current for IR-PMFSG at rated conditions are shown in Figure. 7 under various β_{in} values. Analysis reveals that as soon as β_{in} increases there is slight decrease output current under same design specification thus reducing the stator winding losses. According to the harmonic spectra analysis as shown in Figure. 5(b). It can be clearly seen that 3^{th} and 7^{th} order harmonics decrease whereas 5^{th} order harmonic slightly increases. Due to overall low harmonic contents and reduced THD the resultant torque at rated generating conditions (as shown in Figure. 8) shows small overshoots in its waveform which is caused by insufficient damping of lower circuit resistance. This small damping also caused by higher winding inductance as listed in Table 2.

Comparative analysis of IR-PMFSG and OR-PMFSG in term of the phase back-EMF and output voltage reveals that both generators offer closer output voltage however their open-circuit phase back-EMF greatly varies thus, resulting higher voltage regulation factor in IR-PMFSG which is mainly caused by higher q-axis inductance which cause larger load angle and damping in torque as discussed. In addition, rated operating power for IR-PMFSG is 3399 W whereas for OR-PMFSG is 2297.82 W. This shows that under same specification IR-PMFSG offer 1.47 times power than that of OR-PMFSG.

B. OVERLOAD CAPABILITY

The overload capability of IR-PMFSG and OR-PMFSG with different β_{in} and β_{out} are predicted with FEA based

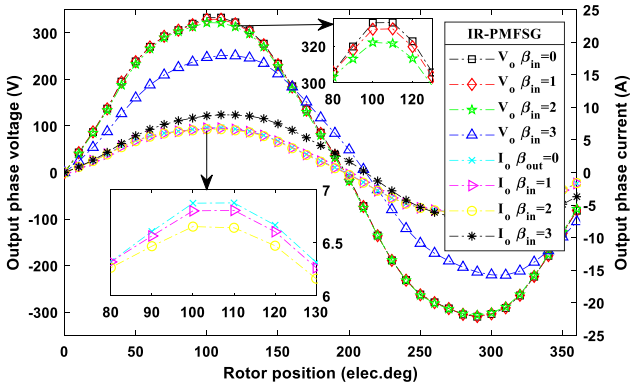

FIGURE 7. Output phase current and phase voltage at rated condition with β_{in}.

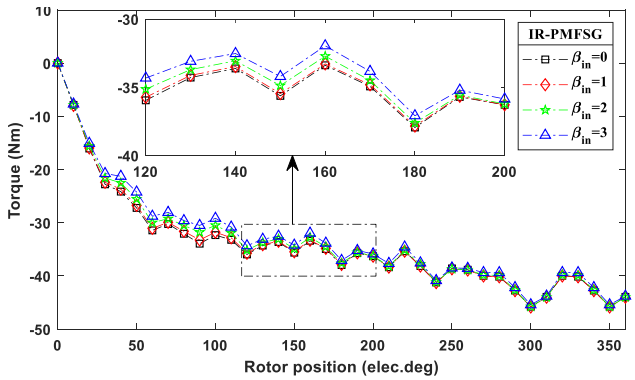

FIGURE 8. Torque at rated generating operation mode with connected rated resistive load @ 1500 rpm.

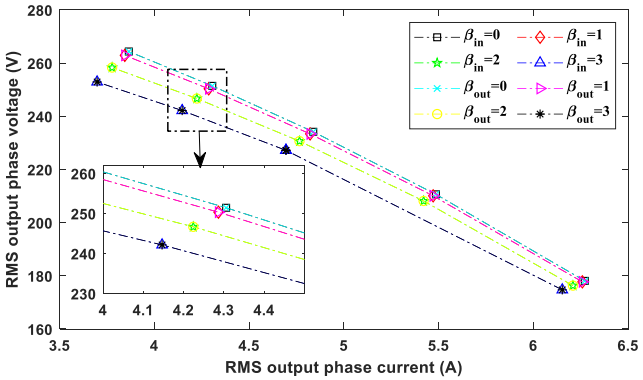

FIGURE 9. Influence of β_{in} and β_{out} on output current and voltage with resistive load range @ 1500 rpm.

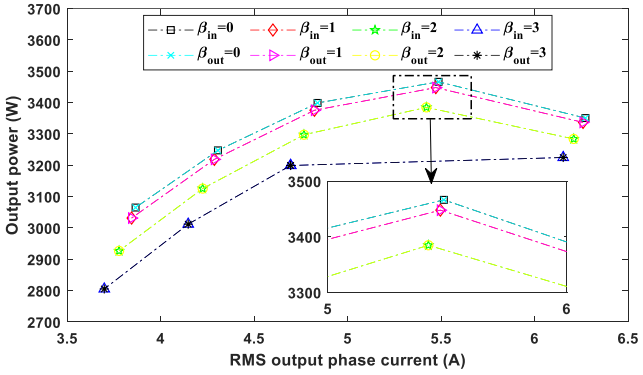

FIGURE 10. Variation of the output power with β_{in} and β_{out} and resistive load range @ 1500 rpm.

co-simulation under various resistive load range at 1500 r/min for output voltage, current, losses which are used for computation of the output power, efficiency and power factor as shown in Figure. 9-12.

Figure. 9 shows RMS values of the output voltage with RMS output current and different β_{in} and β_{out} for IR-PMFSG and OR-PMFSG respectively. Output voltage stability under different resistive load is analyzed from the curve slopes. A detailed investigation reveals that slop of the curve for IR-PMFSG is higher compared to counterpart OR-PMFSG thus indicates higher voltage variation with the resistive load variation resulting higher voltage regulation. Thus, OR-PMFSG exhibits advantages of maintaining more stable voltage in compare with IR-PMFSG at the cost of reduced power as shown in Figure. 10.

The variation of the power level with load levels, β_{in} and β_{out} reveals that maximum operating point for IR-PMFSG is 3399 W whereas for OR-PMFSG it is 2297.82 W. With the introduction of both β_{in} and β_{out} output power are improved slightly. Furthermore, comparison of the rated operating point with specification power (2000 W) shows that in case of OR-PMFSG both rated operating power and specification power are quite close which is 1.15 times whereas in case of IR-PMFSG the rated power is 1.7 times of the specification power. This indicate that IR-PMFSG offer comparatively better overload capability and higher efficiency as shown in Figure. 11. Note that this variation in the overload power capability is mainly due to distinct inductance and respective reactance as listed in Table 2.

Detailed investigation of both β_{in} and β_{out} on loss and efficiency of IR-PMFSG and OR-PMFSG shown in Figure. 11. Analysis reveals that with the introduction of β_{in} and β_{out} in stator core, overall loss reduces due to significant reduction in core loss which results an increase in generator efficiency however resistive load variation shows that as soon as load varies, the corresponding losses increases and decreases generator efficiency. Comparative analysis of efficiency at various load range under overload capability reveals that for IR-PMFSG at rated condition maximum efficiency of 93% is achieved whereas for OR-PMFSG the maximum efficiency obtained in 90.46%. Analysis concludes that IR-PMFSG offers 2.8% higher efficiency.

Similarly, power factor of both IR-PMFSG and OR-PMFSG under various resistive load and β_{in} and β_{out} are analyzed as shown in Figure. 12. It can be clearly seen that for both generator under various conditions, with the increase in the resistive load first drops and then slightly increases. This is because with load variation the corresponding phase

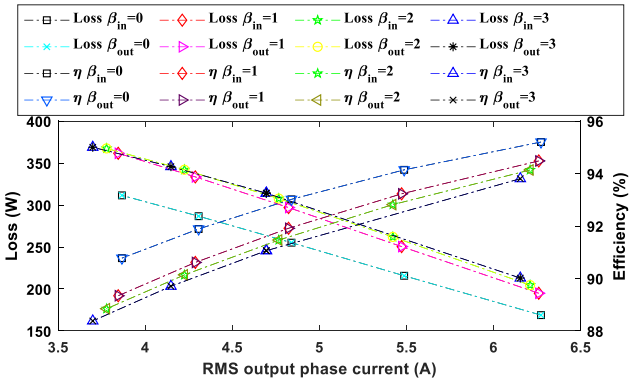

FIGURE 11. Effect of β_{in} and β_{out} on loss and efficiency with resistive load range @ 1500 rpm.

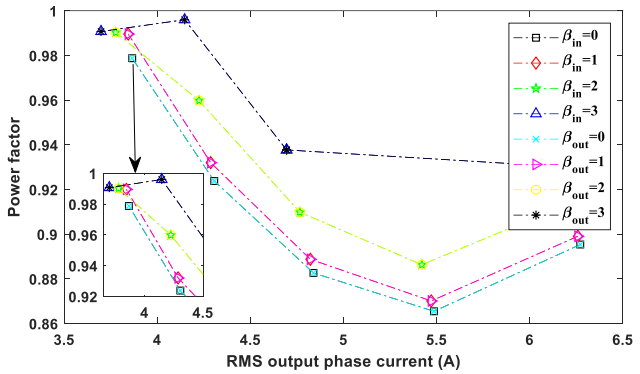

FIGURE 12. Variation of the power factor with β_{in} and β_{out} and resistive load range @ 1500 rpm.

current increases results an increase in reactive power consumption which causes to drop power factor.

C. OVER-SPEED CAPABILITY

Over-speed capability is investigated under rated load (R_{rated}) and various speed before and after rated speed of 1500 rpm. Both IR-PMFSG and OR-PMFSG with β_{in} and β_{out} are investigated in speed range of 1000 to 2000 rpm to thoroughly investigates the influence of speed below and above the rated conditions. In over-speed capability, torque performance when generator is connected to resistive load, output power, losses, and efficiency are investigated as shown in Figure. 13-16.

From Figure. 13 it can be clearly seen that torque profile of both IR-PMFSG and OR-PMFSG with different β_{in} and β_{out} saturates at higher speed whereas it declines slightly after 1600 rpm despite of increase in rotor speed due to increase in the load angle and decrease in q-axis current. Analysis and comparison of the IR-PMFSG and OR-PMFSG reveals that the torque generated at resistive load condition by OR-PMFSG is lower that results a decline in the generated power as shown in Figure. 14. The over-speed power capability shows that IR-PMFSG significantly generate almost 2.25 time of the specification power whereas OR-PMFSG

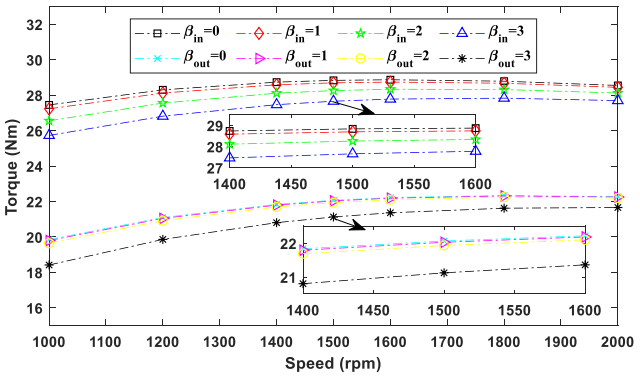

FIGURE 13. Effects of β_{in} and β_{out} on torque with speed connected to resistive load @ R_{rated}.

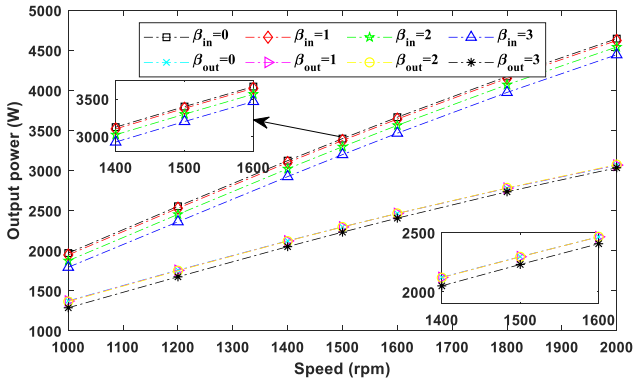

FIGURE 14. Effects of β_{in} and β_{out} on generator output power with speed @ R_{rated}.

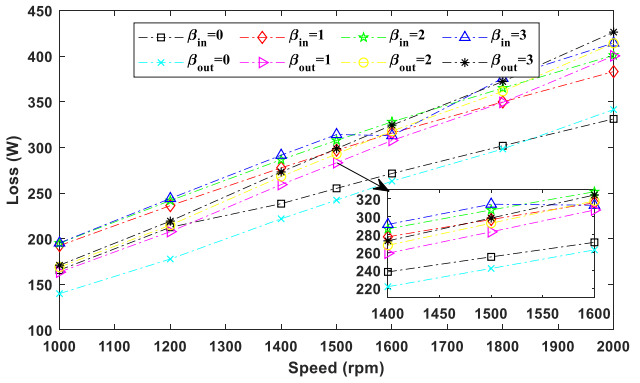

FIGURE 15. Variation of loss with β_{in} and β_{out} and speed @ R_{rated}.

exhibits nearly 1.25 times of the specification power. This analysis concludes that IR-PMFSG can be operated at wide-speed rage for higher power specification requirements.

In over-speed capability the variation of the losses and efficiency in both IR-PMFSG and OR-PMFSG with various β_{in} and β_{out} are illustrated in Figure. 15 and Figure. 16 respectively. Analysis reveals that at lower speed (less than 1200), the overall losses especially core loss for both IR-PMFSG and OR-PMFSG are low despite of variation

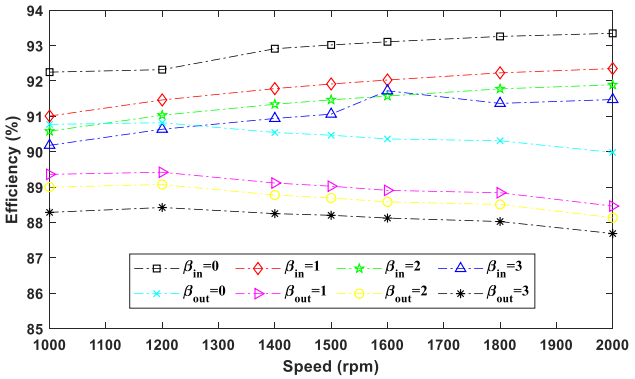

FIGURE 16. Variation of loss with β_{in} and β_{out} and speed @ R_{rated}.

of β_{in} and β_{out} however, at higher speed the losses of IR-PMFSG with $\beta_{in} = 0$ surpasses losses of the OR-PMFSG with $\beta_{out} = 0$ resulting an increase in generator efficiency. Moreover, when $\beta_{in} = 3$ for IR-PMFSG the losses significantly reduce that ultimately increase efficiency at 1600 rpm however, at further increase in the rotor speed losses tent to increase and efficiency decreases. This decrease rate of efficiency in OR-PMFSG is higher than that of IR-PMFSG.

V. CONCLUSION

In this paper two permanent magnet flux switching generator (PMFSG) i.e., inner rotor PMFSG (IR-PMFSG) and outer rotor PMFSG (OR-PMFSG) is designed for 2 kW output power under same specifications and comparatively analyzed for wind power application. Comparative analysis is performed under static characteristics, rated condition, overload capability and over-speed capability for generating output voltage, current, power and efficiency. Static analysis concludes that IR-PMFSG offers 47.93% higher rated power, 2.83% higher efficiency, 22.78% more magnetic flux, 56.91% reduced cogging torque and 83.18% lower torque ripples at the cost of 62.69% higher voltage regulation factor. Rated and overload performance shows that IR-PMFSG exhibits 1.47 times power than that of OR-PMFSG counterpart. In addition, detailed investigation reveals that IR-PMFSG significantly generate almost 2.25 time of the specification power whereas OR-PMFSG exhibits nearly 1.25 times of the specification power under higher rotor speed. Analysis concludes that IR-PMFSG can be operated at wide-speed range for higher power specification requirements maintaining efficiency greater than 90% for wind power generation.

REFERENCES

[1] W. W. E. Association. (Jun. 7, 2016). [Online]. Available: http://www.wwindea.org/the-world-sets-new-wind-installations-record-637gw-new-capacity-in-2015/
[2] L. Shao, W. Hua, F. Li, J. Soulard, Z. Q. Zhu, Z. Wu, and M. Cheng, "A comparative study on nine- and twelve-phase flux-switching permanent-magnet wind power generators," *IEEE Trans. Ind. Appl.*, vol. 55, no. 4, pp. 3607–3616, Jul. 2019.
[3] L. Shao, W. Hua, J. Soulard, Z.-Q. Zhu, Z. Wu, and M. Cheng, "Electromagnetic performance comparison between 12-phase switched flux and surface-mounted PM machines for direct-drive wind power generation," *IEEE Trans. Ind. Appl.*, vol. 56, no. 2, pp. 1408–1422, Mar. 2020.
[4] J. Ojeda, M. G. Simoes, G. Li, and M. Gabsi, "Design of a flux-switching electrical generator for wind turbine systems," *IEEE Trans. Ind. Appl.*, vol. 48, no. 6, pp. 1808–1816, Nov. 2012.
[5] A. S. Thomas, Z. Q. Zhu, and G. W. Jewell, "Comparison of flux switching and surface mounted permanent magnet generators for high-speed applications," *IET Elect. Syst. Transp.*, vol. 1, no. 3, pp. 111–116, Sep. 2011.
[6] F. Li, W. Hua, M. Tong, G. Zhao, and M. Cheng, "Nine-phase flux-switching permanent magnet brushless machine for low-speed and high-torque applications," *IEEE Trans. Magn.*, vol. 51, no. 3, pp. 1–4, Mar. 2015.
[7] Z. Q. Zhu and J. T. Chen, "Advanced flux-switching permanent magnet brushless machines," *IEEE Trans. Magn.*, vol. 46, no. 6, pp. 1447–1453, Jun. 2010.
[8] M. Cheng, W. Hua, J. Zhang, and W. Zhao, "Overview of stator-permanent magnet brushless machines," *IEEE Trans. Ind. Electron.*, vol. 58, no. 11, pp. 5087–5101, Nov. 2011.
[9] W. Zhao, T. A. Lipo, and B. I. Kwon, "A novel dual-rotor, axial field, fault-tolerant flux-switching permanent magnet machine with high-torque performance," *IEEE Trans. Magn.*, vol. 51, no. 11, pp. 1–4, Nov. 2015.
[10] J. Yan, H. Lin, Y. Huang, H. Liu, and Z. Q. Zhu, "Magnetic field analysis of a novel flux switching transverse flux permanent magnet wind generator with 3-D FEM," in *Proc. Int. Conf. Power Electron. Drive Syst. (PEDS)*, Nov. 2009, pp. 332–335.
[11] W. Ullah, F. Khan, and E. Sulaiman, "Sub-domain modelling and multi-variable optimisation of partitioned PM consequent pole flux switching machines," *IET Electr. Power Appl.*, vol. 14, no. 8, pp. 1360–1369, Aug. 2020.
[12] W. K. Ullah, S. Faisal, U. Erwan, U. Muhammad, and K. Noman, "Analytical validation of novel consequent pole E-core stator permanent magnet flux switching machine," *IET Electr. Power Appl.*, vol. 14, no. 5, pp. 789–796, 2020.
[13] W. Ullah, F. Khan, M. Umair, and B. Khan, "Analytical methodologies for design of segmented permanent magnet consequent pole flux switching machine: A comparative analysis," *COMPEL Int. J. Comput. Math. Electr. Electron. Eng.*, vol. 40, no. 3, pp. 744–767, Aug. 2021.
[14] W. Ullah, F. Khan, E. Sulaiman, I. Sami, and J.-S. Ro, "Analytical sub-domain model for magnetic field computation in segmented permanent magnet switched flux consequent pole machine," *IEEE Access*, vol. 9, pp. 3774–3783, 2021.
[15] Z. Q. Zhu, Y. Pang, D. Howe, S. Iwasaki, R. Deodhar, and A. Pride, "Analysis of electromagnetic performance of flux-switching permanent-magnet Machines by nonlinear adaptive lumped parameter magnetic circuit model," *IEEE Trans. Magn.*, vol. 41, no. 11, pp. 4277–4287, Nov. 2005.
[16] Y. Tang, E. Motoasca, J. J. H. Paulides, and E. A. Lomonova, "Comparison of flux-switching machines and permanent magnet synchronous machines in an in-wheel traction application," *COMPEL Int. J. Comput. Math. Electr. Electron. Eng.*, vol. 32, no. 1, pp. 153–165, Dec. 2012.
[17] X. Zhu, Z. Shu, L. Quan, Z. Xiang, and X. Pan, "Design and multicondition comparison of two outer-rotor flux-switching permanent-magnet motors for in-wheel traction applications," *IEEE Trans. Ind. Electron.*, vol. 64, no. 8, pp. 6137–6148, Aug. 2017.
[18] W. Hua, H. L. Zhang, M. Cheng, J. Meng, and C. Hou, "An outer-rotor flux-switching permanent-magnet-machine with wedge-shaped magnets for in-wheel light traction," *IEEE Trans. Ind. Electron.*, vol. 64, no. 1, pp. 69–80, Jan. 2017.
[19] X. Li, S. Liu, and Y. Wang, "Design and analysis of a new HTS dual-rotor flux-switching machine," *IEEE Trans. Appl. Supercond.*, vol. 27, no. 4, pp. 1–5, Jun. 2017.
[20] J. W. Kwon and B. I. Kwon, "Design of novel high performance dual rotor flux-switching drum winding machine," *J. Electr. Eng. Technol.*, vol. 14, pp. 2019–2025, Sep. 2019.
[21] W. Ullah, F. Khan, and M. Umair, "Lumped parameter magnetic equivalent circuit model for design of segmented PM consequent pole flux switching machine," *Eng. Comput.*, vol. 38, no. 2, pp. 572–585, Feb. 2021.
[22] W. Ullah, F. Khan, E. Sulaiman, and M. Umair, "Torque characteristics of high torque density partitioned PM consequent pole flux switching machines with flux barriers," *CES Trans. Electr. Mach. Syst.*, vol. 4, no. 2, pp. 130–141, Jun. 2020.

WASIQ ULLAH (Graduate Student Member, IEEE) is basically from Afghanistan and was born in Peshawar, Khyber Pakhtunkhwa, Pakistan, in 1995. He received the B.S. and M.S. degrees in electrical (power) engineering from COMSATS University Islamabad (Abbottabad Campus), Abbottabad, Pakistan, in 2018 and 2020, respectively, where he is currently pursuing the Ph.D. degree in electrical (power) engineering.

Since 2018, he has been a Research Associate with the Electric Machine Design Research Group. His research interests include analytical modeling, design analysis and optimization of permanent magnet flux switching machines, linear flux switching machines, hybrid excited flux switching machines, and novel consequent pole flux switching machines for high-speed brushless ac applications.

Mr. Ullah is a Graduate Student Member of the IEEE-IES and a member of the Pakistan Engineering Council.

FAISAL KHAN (Member, IEEE) was born in Charsadda, Khyber Pakhtunkhwa, Pakistan, in 1986. He received the B.S. degree in electronics engineering and the M.S. degree in electrical engineering from COMSATS University Islamabad (Abbottabad Campus), Pakistan, in 2009 and 2012, respectively, and the Ph.D. degree in electrical engineering from the Universiti Tun Hussein Onn Malaysia, Malaysia, in 2017.

From 2010 to 2012, he was a Lecturer with the University of Engineering and Technology, Abbottabad, Pakistan. Since 2017, he has been an Assistant Professor with the Electrical and Computer Engineering Department, COMSATS University Islamabad (Abbottabad Campus). He is the author of more than 100 publications, one patent, and received multiple research awards. His research interests include design and analysis of flux-switching machines, synchronous machines, and dc machines.

Dr. Khan is a member of the IEEE-IES Electrical Machines Technical Committee.

SHAHID HUSSAIN (Graduate Student Member, IEEE) was born in Swabi, Khyber Pakhtunkhwa, Pakistan. He received the B.S. degree in electrical power engineering from COMSATS University Islamabad, Abbottabad Campus, Abbottabad, Pakistan, in 2019. He is currently pursuing the M.S. degree in electrical power engineering with COMSATS University Islamabad (Abbottabad Campus).

Since 2020, he has been a Research Assistant with the Machine Design Group. His research interests include design analysis, optimization and experimental validation of modular and complementary fault tolerant field excited linear flux switching machines for long stroke application. He is a member of the Pakistan Engineering Council.